Fifth-generation small cell backhaul capacity enhancement and large-scale parameter effect

Olabode Idowu-Bismark, Francis Idachaba, Aderemi A. Atayero
Electrical and Information Engineering Department, Faculty of Engineering, Covenant University, Ota, Nigeria

Article Info	ABSTRACT
	The proliferation of handheld devices has continued to push the demand for higher data rates. Network providers will use small cells as an overlay to macrocell in fifth-generation (5G) for network capacity enhancement. The current cellular wireless backhauls suffer from the problem of insufficient backhaul capacity to cater to the new small cell deployment scenarios. Using the 3D digital map of Lagos Island in the Wireless InSite, small cells are deployed on a street canyon and in high-rise scenarios to simulate the backhaul links to the small cells at 28 GHz center frequency and 100 MHz bandwidth. Using a user-defined signal to interference plus noise ratio-throughput (SINR-throughput) table based on an adaptive modulation and coding scheme (MCS), the throughput values were generated based on the equation specified by 3GPP TS 38.306 V15.2.0 0, which estimates the peak data rate based on the modulation order and coding rate for each data stream calculated by the propagation model. Finding shows achieved channel capacity is comparable with gigabit passive optical networks (GPON) used in fiber to the 'X' (FTTX) for backhauling small cells. The effect of channel parameters such as root mean squared (RMS) delay spread and RMS angular spread on channel capacity are also investigated and explained. *This is an open access article under the <u>CC BY-SA</u> license.*

Corresponding Author:

Olabode Idowu-Bismark
Department of Electrical and Information Engineering, Faculty of Engineering, Covenant University
Canaan Land Ota, Nigeria
Email: idowubismarkolabode@gmail.com

1. INTRODUCTION

The requirement of the fifth generation (5G) communication paradigm is diverse according to [1]. It includes over 20 Gbps peak data rate with a latency of 1 ms, spectrum efficiency of 3x that of 4G and up to 5x in hot spots, as well as extensive connectivity of machine type devices for machine-to-machine (M2M) communication and a host of other requirements. It has been suggested in [2] that network densification (ND) is a method to achieve the need for 5G. ND is the deployment of small cells (picocells, and femtocells) as an overlay in macrocell with massive multiple-input, multiple-output (MIMO) and mmWave (30 to 300 GHz) band at the base station and or the user equipment. Small cells in ultra-dense network (UDN) link with the network via a backhaul connection to macrocell base station (BS). This backhaul of dense small cell networks has emerged as a bottleneck of their successful deployment, particularly for the last-mile link. There is other backhaul technologies with different capabilities available to small cell networks. Generally, backhaul links are either wired or wireless technologies. The wired backhaul includes copper used in the digital subscriber line and optic fiber with last-mile technology being Fiber-to-the-X where 'X' could stand for H-home, B-building, to form fiber-to-the-home (FTTH), and fiber-to-the-building (FTTB). The last-mile wireless backhaul is mobile wireless which includes the third-generation (3G) high-speed packet access (HSPA+), fourth-generation (4G) long term evolution (LTE), and wireless fidelity (Wi-Fi) [3]. Optic fiber cables are

either ideal with very high throughput and very low latency, i.e., fiber access 4, or non-ideal with moderate throughput and latency, i.e., fiber 1 to 3. Unlike the wired backhaul, the wireless backhaul is always non-ideal [4]. However, it might be a feasible solution in hyper-dense networks since wired backhaul poses a problem for the last-mile link. This problem is due to many small cells and their incremental, unplanned deployment leading to high cost, issues with right of way, and a long time to deployment [5]. The use of wireless backhaul for small cells requires a high data rate that mmWave frequencies can offer due to its availability of broader bandwidth. However, its implementation has significant issues, including high pathloss, severe penetration loss, and its resulting channel being poorly scattered [6], [7]. The use of massive MIMO combined with mmWave for backhaul employing beamforming at the BS offers solutions to solve the above challenges [8]. There are many ways to facilitate the 5G wireless UDN based on mmWave massive MIMO. One such architecture used for the 5G network is shown in Figure 1. The sizeable accessible bandwidth and the high spectral efficiency qualify the mmWave massive MIMO as a potential technology choice to enhance the ongoing 5G cellular network overall system throughput [9].
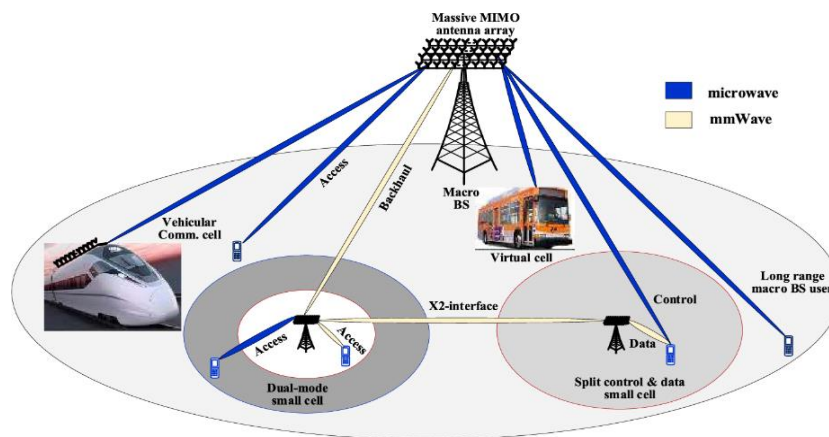

Figure 1. mmWave massive MIMO architecture for enhanced backhaul in 5G [10]

Small cells are multi-radio access technologies (multi-RAT) capable and represent an essential part of the UDN, which are considered an imperative 5G solution. Sharing the spectrum in a UDN requires intelligent inter-cell interference coordination, cancellation, or exploitation [11]. Moreover, the small cells feature different capabilities, transmission powers, coverage, and deployment scenarios [12]. Backhauling is data evacuation from the base station to the core network. One deployment scenario for last-mile application for optic fiber is the fiber to the 'X' (FTTX), which uses the active optical network (AON) or passive optical network (PON). As a result of its cost-effectiveness for multiple connections to homes and small business enterprises (SMEs), the PON technology is globally used for fiber optic last-mile internet connections [3]. Gigabit passive optical networks (GPON), a gigabit per second speed version of the PON, is an optical system for the access networks based on ITU-T specifications G.984 series [13]. It can provide a 20 km reach with a 28 dB optical budget by using class B+ optics with a 1:32 split ratio. GPON system supports 155 Mbps upstream and 1.24 Gbps downstream up to 1.24 Gbps upstream and 1.24 Gbps downstream, and 155 Mbps upstream and 2.49 Gbps downstream up to 2.49 Gbps upstream and 2.49 Gbps downstream. GPON supports both asynchronous transmission mode (ATM) and GPON encapsulation method (GEM) encapsulation. GPON encapsulation method supports native time division multiplexing (TDM) and data [14]. Table 1 shows transmission rates of different PON technologies.

Table 1. Transmission rates of different PON technologies [3]

Parameter	EPON	GPON	10G EPON	10G GPON
Standard	IEEE 802.3ah	ITU-T G.984	IEEE.802.3av	ITU-T G.987
Rate (Gbps)	1.25/1.25	1.2/2.4	1/10	2.5/10
Fiber type	SM (ITU-T G.652)	SM (ITU-T G.652)	SM (ITU-T G.652)	SM (ITU-T G.652)
Max distance reach (OLT-ONU)	10 km/20 km	20 km	10 km/20 km	20 km

Different small cells wireless backhaul methods are based on the frequency band of choice. There is the in-band backhaul, otherwise called self-backhauling, and the out-of-band backhaul. Ni *et al.* [15] and

Ge *et al.* [16], even within these two methods, there are many topologies. Also, small cells in UDN are expected to be deployed incrementally without detailed network planning. Some may not find a direct backhaul to the core network, thus requiring one or two other small cells to create a multi-hop backhaul link that will forward its traffic to a nearby small cell to reach a node that can connect it with the core network [17]. Based on the above considerations, three topologies exist; single gateway node, where the small cells handle their traffic and accumulate traffic for the small cells along the branches of the tree that are probably out of the LOS of the macrocell. Next is the multiple gateway nodes (MGN), a multi-root tree topology. MGN is to provide an alternative gateway node for backhauling if a gateway node is inaccessible or down. Finally, we have the Mesh and Redundancy in Loops topology. The mesh topology gives occasions to attain redundancy in loops such that a node has multiple routes to reach the gateway node, thereby improving the reliability of the backhaul network. Routing is a crucial aspect of the topology, and developing routing schemes that maximize the overall throughput of the backhaul network is critical [16].

In [18]–[20] have carried out work to investigate the characteristics of mmWave massive MIMO channel for backhaul and how the channel parameters impact various capabilities of the wireless channel, including the channel capacity. According to [18], the UDN is an expected promising candidate to be deployed for the ongoing 5G networks to achieve the high data rate demand. However, to realize this UDN, a vital precondition is a dependable, cost-effective, large gigahertz bandwidth backhaul link between ultra-dense small cell base stations (SC BSs) and macrocell BS. The authors then suggested using mmWave massive MIMO for enhanced link reliability. The paper proposed a digitally controlled phase shifter network (DPSN) based hybrid precoding/combing scheme. Similar to [18] is the work conducted by Nakamura *et al.* [19]. They study interference management for mmWave mesh backhaul networks using orthogonal channel allocation and optimal transmission allocation. Their result shows that the backhaul bottleneck due to interference was reduced, increasing throughput. Feng and Mao [20], a deep reinforcement learning algorithm, managed and improved the limited backhaul capacity of the mmWave communication system between the BS and the core network. The backhaul capacity improvement was achieved through efficient resource allocation. In [21], the authors performed a performance analysis for the mmWave integrated access and backhaul between small cells and the macrocell base station. They derive the downlink rate coverage probability for different resource allocations at the macrocell BS. The result analysis of the downlink rate coverage probability shows that offloading users from the macrocell BS to small cell BSs improves the obtained rate as compared to HetNet with fiber-backhauled small cell. The works of [22] use Winpro 3D ray-tracing software to compute throughput, maximum data rate, and capacity improvement due to MIMO beamforming. The authors used the Winpro software to simulate mmWave MIMO for small cell wireless backhaul and access data rate limitations. They showed that a peak data rate of 15 Gbps is possible with a cell edge rate above 400 Mbps. Varzakas [23], characterized a hybrid direct-sequence slow frequency hopping code-division multiple access (CDMA) system in the Rayleigh fading environment, and the channel capacity achievable per user-determined.

In this paper, the authors proposed a novel use of a 5G new radio (5G NR) air interface employing closed-loop diversity to provide optimal performance for the wireless backhaul link of small cells to BS. The authors used an adaptive modulation and coding scheme which helps maintain a constant throughput over a wide range of user equipment/small cells, thereby providing a backhaul link with the required capacity for small cells. The three main contributions of this work are: i) development of three-dimensional beamforming (3DBF) backhaul link capable of Gbps channel capacity comparable with optic fiber (GPON/2.4 Gbps) using ray-tracing simulation techniques, thus making it suitable for last-mile backhaul of small cells in place of optic fiber; ii) provision of models for the effect of large-scale channel parameters on the backhaul link capacity suitable for predicting network deployment in an urban high-density high-rise and street canyon environment of Lagos Island and a similar environment; and iii) the cross-correlation coefficient results of this research engender an accurate comparison between the large scale parameters (LSPs) and their effect on the backhaul link channel capacity, particularly during network optimization. The rest of this paper is organized as follows: section 2 provides the research method's details, and section 3 presents the results and discussions. We conclude in section 4.

2.   METHOD

Explaining this section considers the various equipment, tools, and methods used in the experiment's simulation, their attributes, and specifications. These include the BS and small cell specifications, the Remcom Wireless InSite software, the MATLAB 2017b, and the digital 3D map used in this work. Lately, two frequency bands have been suggested as good candidates for wireless backhaul. These are the current cellular frequency band and the mmWave, such as 28 GHz, 60 GHz, and, E-band ranging from 71 to 76 GHz and 81 to 86 GHz [24]. One of the predominant frequency ranges for the 5G NR as proposed by the 3GPP TR 138 901 release 15 of 2018 [25] is the 24.25 to 29.5 GHz. Also, since atmospheric attenuation for mmWave is near the lowest at 28 GHz [26]. These necessitate the proposed carrier frequency of 28 GHz, while the bandwidth of 100 MHz

is the minimum channel bandwidth for all carrier frequencies as specified in the 3GPP release 15 standards [25]. Since mmWave suffers from high propagation loss, it is best suited for short-distance transmission such as short-distance wireless backhauls among SCs.

In this work, the authors define the channel signal quality using the channel's signal to interference plus noise ratio (SINR). This is done by putting together a user-defined SINR-throughput table as shown in Table 2 using the adaptive modulation and coding scheme (MCS) in Wireless InSite, a map-based deterministic commercial simulation tool. The throughput values were generated based on the equation specified by 3GPP TS 38.306 V15.2.0 0, which estimates the peak data rate based on the modulation order and coding rate for each data stream calculated by the propagation model. Table 3 shows the simulations parameter and their values.

Table 2. SINR-throughput lookup tables for simulation

SINR (dB)	Throughput (Mbps)	MCS
0.21	53.87	QPSK_0.40
4.54	101.01	QPSK_0.75
6.94	107.74	QPSK_0.80
8.48	134.68	QPSK_1.00
10.84	202.02	16QAM_0.75
12.41	215.48	16QAM_0.80
13.78	269.36	16QAM_1.00
16.46	303.02	64QAM_0.75
18.15	323.23	64QAM_0.80
26.0	404.03	256QAM_0.75
27.5	430.97	256QAM_0.80
33.3	538.71	256QAM_1.00

Table 3. Simulation parameters

Simulation parameters	Values
Number of street small cells	596
Number of high-rise small cells	30
Carrier frequency	28 GHz
Bandwidth	100 MHz
BS transmit power	30 dBm
BS height	10 m
Street small cell height	2.5 m
High-rise small cell height	Various
Antenna configuration	
BS Antenna	4×4 UPA
Small cell antenna	2×2
Antenna element spacing	1 wavelength

The BS utilizes the 4×4 dual-polarized MIMO uniform planar antenna array (UPA) with a half-wave dipole and one wavelength spacing between elements for the simulation's communication system. The BS is located at 10 m within Tinubu Square at Lagos Island, Nigeria, and uses a maximum ratio transmission algorithm and adaptive modulation. In the first scenario, 596 small cells receivers are located along broad street, a street canyon environment. The second scenario has 30 small cells vertically located on a 30-story building to create the high-rise scenario. The small cell receivers use a 2×2 MIMO antenna array operating at 28 GHz carrier frequency and 100 MHz bandwidth. Maximal ratio combining is used at the receiver to model the receiver diversity. The channel vectors of the H-matrix are used to adjust the magnitudes and phases of the MIMO antenna elements to maximize the total received power. A 3D digital map of Lagos Island is uploaded to the Wireless InSite ray-tracing software to create the propagation environment. A narrowband sinusoidal 28 GHz waveform with a bandwidth of 100 MHz is generated, then used to create a 4×4 dual-polarized MIMO transmitter antenna and 2×2 MIMO receiver antenna. After the simulation, the extracted output dataset for the backhaul channel capacity, angular spread of arrival and departure in the azimuth and elevation domain, and were post-process in MATLAB.

3.   RESULTS AND DISCUSSION

After the simulation, data generated were processed and the results obtained analyzed. In this section, the analysis of the results was explained. The achievable data rate for the street canyon and high-rise scenarios were presented while the effect of large-scale parameters was also explained.

3.1. Channel capacity for high-rise

In the high-rise scenario, the first three floors were in an outage. The above indicates mmWave susceptibility to blockage and the need for more than one BS to cover high-rise buildings in mmWave-based cellular networks. The result shows a gradual increase in the channel capacity as the building height increases to a peak at 1.42 Gbps on the 9th floor and then decreases gradually to about 0.72 Gbps on the 30th floor. Meanwhile, the throughput for high-rise shows a reasonably constant value between 500 to 300 Mbps per floor/small cell. Table 4 shows values of channel capacity for selected high-rise floors. Figure 2 shows the normal distribution of channel capacity for a high-rise scenario.

3.2. Channel capacity for street canyon

For the street scenario, the record shows a channel capacity value of about 1.8 to 2.0 Gbps for the small cells close to the BS, which gradually decreases as we move towards the far end, with capacity dropping to about 0.4 Gbps at 590 m. At 200 m, we see a channel capacity of 1.14 Gbps and a throughput of 430 Mbps.

Table 5 shows channel capacity values for selected small cells between 5 to 200 m. Figure 3 is the probability distribution of the street canyon small cells channel capacity showing a lognormal distribution. Compared with other candidate technologies for the last-mile backhaul of small cells, the proposed 5G NR backhaul offers link capacity comparable with optic fiber capacity, as seen in Table 6.

Table 4. Channel capacity for selected high-rise floors

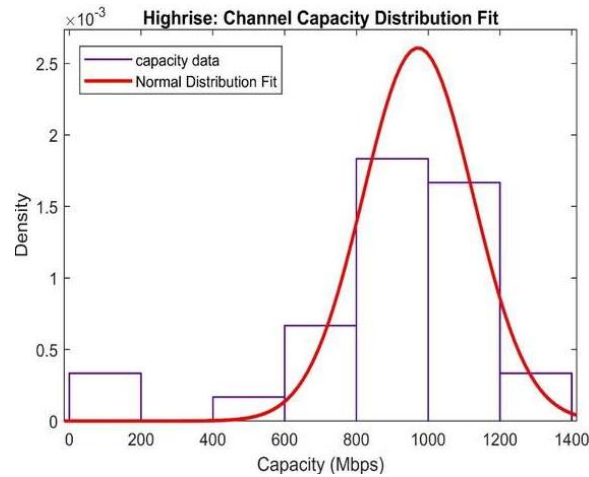| Floor No	Capacity (Mbps)	Throughput (Mbps)
1st	0.12	0
2nd	0.082	0
3rd	695.23	323.23
5th	519.01	269.36
7th	1011.73	430.97
10th	1194.09	538.71
12th	1109.98	538.71
15th	1075.26	430.79
17th	1024.85	430.97
20th	919.69	430.79
22nd	875.37	404.03
25th	867.79	404.03
27th	857.19	323.23
29th	796.57	404.03
30th	723.89	323.23

Figure 2. Pdf of channel capacity for high-rise

Table 5. Channel capacity for street canyon

| Distance (m)	Capacity (Mbps)	Throughput (Mbps)
10.00	1852.31	538.71
20.00	1758.87	538.71
30.00	1734.57	538.71
40.00	1541.03	538.71
50.00	1501.09	538.71
60.00	1447.86	538.71
70.00	1495.53	538.71
80.00	1357.93	538.71
90.00	1356.18	538.71
100.00	1242.56	538.71
110.00	1228.76	538.71
120.00	1277.64	430.97
130.00	1241.46	538.71
140.00	1232.69	538.71
150.00	1321.61	538.71
160.00	1060.44	538.71
170.00	1240.62	538.71
180.00	1194.46	430.97
190.00	1031.96	430.97
200.00	1138.24	430.97
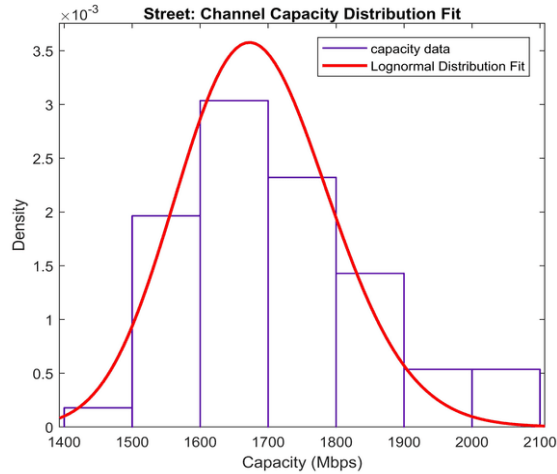
Figure 3. Pdf of channel capacity for street canyon scenario

Table 6. Comparison of candidate backhaul technologies with the proposed 5G NR link

Technology	Standard	Frequency/Wavelength	Multiplexing	Rate	Usage
EPON	IEEE 802.3ah	1260 to 1360 nm 1480 to 1500 nm	WDM	1.25/1.25 Gbps	FTTX
10G EPON	1EEE 802.3av	1577 nm 1270 nm	WDM	10/1 Gbps	FTTX
GPON	ITU-T G.984	1290 to 1330 nm 1480 to 1500 nm	WDM	2.4/1.2 Gbps	FTTX
10GPON	ITU-T G.987	1577 nm 1270 nm	WDM	10/2.5 Gbps	FTTX
WiMAX	IEEE 802.16d/m	2 to 11 GHz	OFDM	75 Mbps	Fixed and Mobile BWA
3.9G	LTE	2 to 3.5 GHz	OFDM and OFCDM	200 Mbps	Mobile BWA
4G	LTE-A	2 to 3.5 GHz	OFDM and OFCDM	1 Gbps	Mobile BWA
Proposed	5G NR	28 GHz	OFDM and NOMA	Street canyon: 2 Gbps at 5 m 0.75 Gbps at 500 m High-rise: 1.24 Gbps at 252 m 0.72 Gbps at 271 m	Fixed and Mobile BWA

Table 7 compares the channel capacity statistics for the high-rise and street canyon scenarios. The minimum achievable rate for the high-rise (0.08 Mbps) was as a result of outages at the lower floors due to blockages of the mmWave signals from the BS. However, it is shown that a high-rise scenario can achieve a considerable amount of channel capacity in the order of Gbps.

Table 7. Comparison between channel capacity statistics for high-rise and street canyon scenarios

	HIGH-RISE (Mbps)	STREET CANYON (Mbps)
Min capacity	0.08	87.90
Max capacity	1240.19	2040.00
Mean	892.03	965.45
10% percentile	515.00	1520.00
50% percentile	920.00	1680.00
90% percentile	1200.00	1840.00

The research result shows that the obtained channel capacity in both scenarios is considerably higher than LTE/LTE-A channel capacity, which stood at 1 Gbps maximum. The simulation achieved 2 Gbps for the street canyon scenario and 1.24 Gbps for the high-rise scenario. The throughput values show that the data rate can sustain a multi-hop small cell network. Compared with the wired GPON and 10GPON technology, the result faired favorable, particularly if we consider that both the GPON and 10GPON rates are composite for at least 16 users. Thus, GPON and 10GPON give a downlink/uplink per-user rate of 150/75 Mbps for GPON and 625/62.5 Mbps for 10GPON, which are lower than this work per-user rate. Adaptive modulation and coding in this work enable higher and constant backhaul link throughput. A throughput of 538.71 Mbps at 200 m was

achieved in the street canyon scenario, with 407.73 Mbps in the high-rise scenario except where there was an outage. The above shows that with our result, the proposed backhaul link has a better capacity than the current LTE/LTE-A and compares favorably with the 10GPON state-of-the-art wired backhaul.

3.3. Effect of large-scale parameters on channel capacity

This section considers the impact of elevation domain large-scale parameters on channel capacity. Such large-scale parameters include the root mean squared delay spread and the root mean squared angular spread. The large-scale parameter's behavior in the azimuth and elevation domain at the arrival and departure respectively were also considered.

3.3.1. Effect of root mean squared delay spread on channel capacity

Considering the behavior of the channel capacity with the root mean square delay spread (RMS DS) as the height of the building increases, a decrease in the channel capacity is observed as the RMS DS increases. Each point in Figure 4 represents a relationship between delay spread and channel capacity of each floor. Some points (represented by x) were excluded from Figure 4 to get an exact fit for the curve. The above is because the first three floors were in an outage in the high-rise scenario, and their results are unreliable and, thus, can be considered outliers. Their exclusion shows the effect of RMS DS on capacity as a negative linear relationship where channel capacity decreases with an increase in RMS DS.

Further examination shows the arrival of three arriving clusters. Generally, a cluster is regularly referred to as a resolvable multipath component (MPC) or a group of MPCs propagating together in delay and space domains having similar departure and arrival angles [27]. The first arriving cluster covers the lower part of the building Figure 4 between the 1st to 12th floor and has the highest channel capacity between 1 Gbps to 1.2 Gbps with the lowest delay spread of between 0 to 100 ns. The second arriving cluster covers the 13th to 22nd floor with a capacity of 0.9 Gbps to 1.1 Gbps and a delay spread of between 170 to 250 ns. The last arriving cluster covers the 23rd floor to the 30th floor with a channel capacity range of between 0.8 to 0.9 Gbps, and the highest values of delay spread between 350 to 400 ns. The model is denoted by (1).

$$f(x) = -0.76x + 948 \tag{1}$$

In the street canyon scenario, we see a decrease in the channel capacity as the RMS DS increases, just as seen in the case of the high-rise. It is also noticed that the delay spread close to the BS is minimal because the SCs are close to the BS, and the distance traveled by the multipath components is very short, leading to small values of delay spread. As we move away from the BS, the delay spread values increase with an increase in the BS-UE distance. The multipath components traveled longer distances, leading to a corresponding decrease in channel capacity. Figure 5 shows the range of the delay spread increasing as channel capacity decreases where at 33 ns, we have about 1.9 Gbps, at 75 ns, the capacity has decreased to about 1.3 Gbps, and finally, at 117 ns, we have a channel capacity of approximately 0.5 Gbps. The effect of RMS DS on the channel capacity for the street canyon scenario can thus be represented by the second-order polynomial in (2).

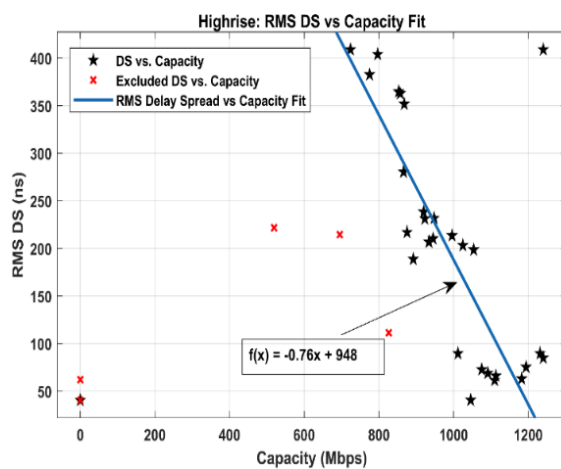$$f(x) = 0.00035x^2 - 0.000000000169x + 0.000000228 \tag{2}$$

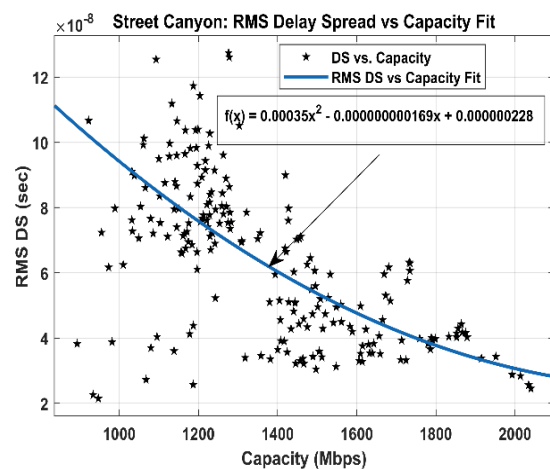Figure 4. RMS DS vs. capacity for high-rise   Figure 5. RMS DS with capacity street

3.3.2. Effect of root mean squared elevation spread of arrival on channel capacity

The effect of root mean squared elevation spread of arrival (RMS ESA) on channel capacity is reviewed in this section. In the high-rise scenario, Figure 6, we see ESA increasing with channel capacity correspondingly decreasing along with the height of the building, where at 5° ESA, the channel capacity was at 1.18 Gbps. As the ESA increases to 10°, channel capacity decreases to 0.95 Gbps. At the top of the building where ESA figures were highest, a 25° ESA corresponds to a capacity value of about 0.35 Gbps. The relationship is represented by (3).

$$f(x) = -0.0236x + 33.61 \tag{3}$$

In the street canyon scenario, ESA decreases rapidly with channel capacity, as shown in Figure 7 (with ESA at about 17° and channel capacity at 2 Gbps near the BS, both decrease with distance). This ESA decrease with channel capacity seems to contradict the belief that reducing angular spread increases channel capacity. However, we should consider that the highest channel capacity was achieved very close to the BS, where we have a lot of scatters leading to the large value of ESA. However, the effect of the large value of ESA was overshadowed by the ample BS power giving rise to large channel capacity. As the BS-UE distance increases and the UE enters the wave guide-like street canyon, the value of ESA slowly decreases before becoming relatively constant. The decrease in channel capacity can be attributed more to pathloss than RMS ESA. The RMS ESA relationship with channel capacity is modeled by (4).

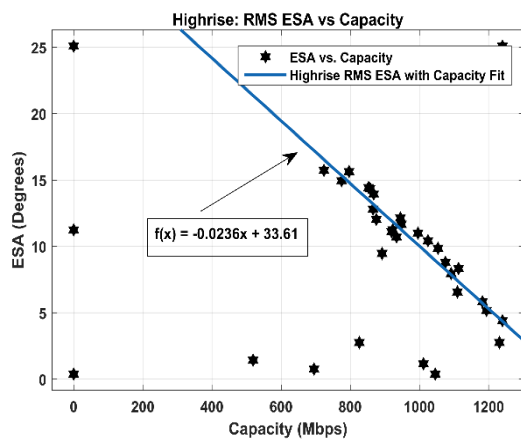$$f(x) = 0.000028x^2 - 0.073x + 48.83 \tag{4}$$
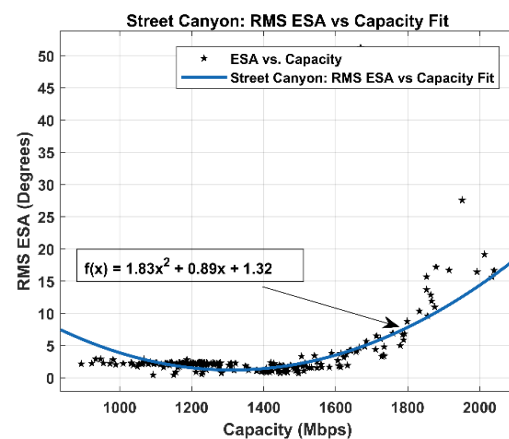

Figure 6. RMS ESA with capacity for high-rise

Figure 7. RMS ESA with capacity for street canyon

3.3.3. Effect of RMS ESD on channel capacity

The exact relationship observed in the RMS ESA with channel capacity is repeated in the case of RMS ESD with channel capacity, as Figure 8 for high-rise shows an ESD value of 5°, corresponding to about 1.2 Gbps. As ESD increases to 15° channel capacity decreases to about 1.05 Gbps. Figure 9 for the street canyon scenario shows that at about 20 ESD, the channel capacity was at 1 Gbps while the value increased as the ESD increased. At 7.5°, the channel capacity has risen to about 2 Gbps. The models for the high-rise and street canyon scenarios are represented by (5) and (6), respectively.

$$f(x) = -0.08x + 105 \tag{5}$$

$$f(x) = 0.55x^2 + 0.93x + 0.87 \tag{6}$$

3.4. Cross-correlation coefficient of LSPs with capacity

Understanding the behavior of the parameters and their distribution functions is essential. Still, the knowledge of the cross-correlation between them is also of pronounced interest, and we can leverage this knowledge for more realistic channel simulations. The cross-correlation coefficient is vital for analyzing the collective behavior of the parameters. Table 8 is the cross-correlation coefficients for angular spread and delay spread with channel capacity. There is no literature precedence to validate the values of channel capacity

cross-correlation coefficient with LSPs. Still, we believe in the integrity of our result and hope it will be the basis for further research by other scholars.
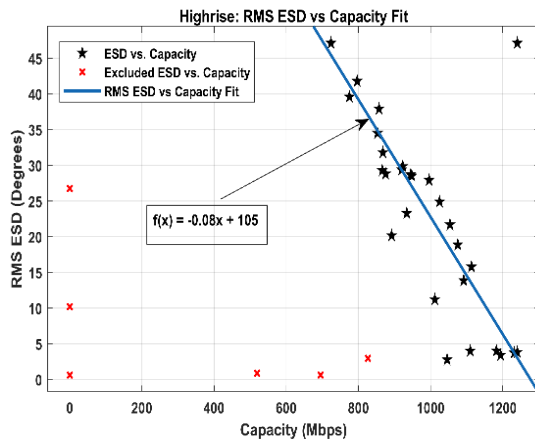

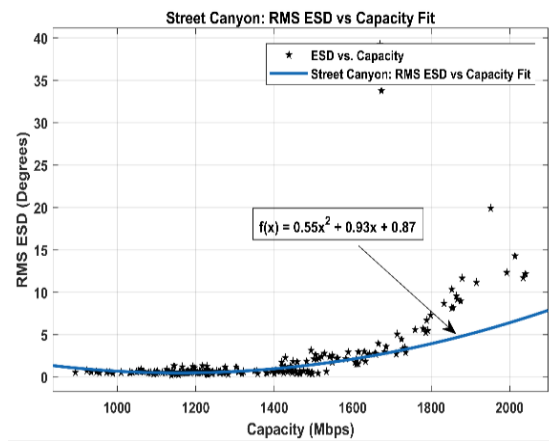Figure 8. RMS ESD with capacity for high-rise

Figure 9. RMS ESD with capacity for street

Table 8. Cross-correlation coefficients for RMS AS and RMS DS with channel capacity

	Urban high-density high-rise (O2I)	Street canyon (UMi)
Capacity vs. RMS DS	-0.10	-0.22
Capacity vs. RMS ASA	0.10	0.23
Capacity vs. RMS ASD	-0.14	-0.31
Capacity vs. RMS ESA	-0.46	0.36
Capacity vs. RMS ESD	-0.17	0.22

4. CONCLUSION

The need for last mile wireless backhauls for small cells in UDN and the inability of the current LTE/LTE-A to meet the data rate requirement led to the proposed simulated backhaul link. The simulated link shows the ability for Gbps channel capacity in areas where the deployment of optic fiber cables poses a challenge. The use of adaptive modulation and adaptive coding enabled the achievement of higher and stable throughput of 538.71 Mbps throughout the cell coverage of 200 m for the street canyon scenario and 407.73 Mbps for the high-rise scenario. These values are higher than obtained for the state-of-the-art wireless backhaul (LTE/LTE-A) and are comparable with the wired backhaul (GPON, 10GPON) channel capacity. The scope of this work is limited to the backhaul link, while the access link is not considered. While 100 MHz bandwidth is used in this work, the research direction is considering higher bandwidth in the order of GHz for greater data rate used for applications such as virtual reality, where a single user may require 250 Mbps connection speed. Models of the effect of large-scale parameters on the channel capacity of the backhaul link were also produced. These are suitable for predicting network deployment. It is expected that the authors of this work will perform future simulations for city-wide coverage for better prediction.

REFERENCES

[1] H. Ullah, N. G. Nair, A. Moore, C. Nugent, P. Muschamp, and M. Cuevas, "5G communication: An overview of vehicle-to-everything, drones, and healthcare use-cases," *IEEE Access*, vol. 7, pp. 37251–37268, 2019, doi: 10.1109/ACCESS.2019.2905347.

[2] O. Idowu-Bismark, F. Idachaba, and A. A. Atayero, "Large-scale parameter modelling for millimeter-wave multiple-input multiple-output channel in 5G ultra-dense network," *Indonesian Journal of Electrical Engineering and Computer Science (IJEECS)*, vol. 26, no. 2, pp. 794–807, May 2022, doi: 10.11591/ijeecs.v26.i2.pp794-807.

[3] O. E. Agboje, S. O. Adedoyin, and C. U. Ndujiuba, "State of fiber optic networks for internet broadband penetration in Nigeria - a review," *International Journal of Optoelectronic Engineering*, vol. 7, no. 1, pp. 1–12, 2017.

[4]   M. Kamel, W. Hamouda, and A. Youssef, "Ultra-dense networks: a survey," *IEEE Communications Surveys and Tutorials*, vol. 18, no. 4, pp. 2522–2545, 2016, doi: 10.1109/COMST.2016.2571730.

[5]   S. Saadat, D. Chen, and T. Jiang, "Multipath multihop mmWave backhaul in ultra-dense small-cell network," *Digital Communications and Networks*, vol. 4, no. 2, pp. 111–117, Apr. 2018, doi: 10.1016/j.dcan.2017.08.002.

[6]   M.-C. Lee and W.-H. Chung, "Transmitter design for analog beamforming aided spatial modulation in millimeter wave MIMO systems," in *2016 IEEE 27th Annual International Symposium on Personal, Indoor, and Mobile Radio Communications (PIMRC)*, Sep. 2016, pp. 1–6, doi: 10.1109/PIMRC.2016.7794712.

[7]   O. Idowu-Bismark, O. Oyeleke, A. A. Atayero, and F. Idachaba, "5G small cell backhaul: A solution based on GSM-aided hybrid beamforming," *International Journal of Computer Network and Information Security*, vol. 11, no. 8, pp. 24–31, Aug. 2019, doi: 10.5815/ijcnis.2019.08.03.

[8]   S. Alabed, I. Maaz, and M. Al-Rabayah, "Distributed differential beamforming and power allocation for cooperative communication networks," *International Journal of Electrical and Computer Engineering (IJECE)*, vol. 10, no. 6, pp. 5923–5931, Dec. 2020, doi: 10.11591/ijece.v10i6.pp5923-5931.

[9]   Y. Liu, C.-X. Wang, J. Huang, J. Sun, and W. Zhang, "Novel 3-D nonstationary MmWave massive MIMO channel models for 5G high-speed train wireless communications," *IEEE Transactions on Vehicular Technology*, vol. 68, no. 3, pp. 2077–2086, Mar. 2019, doi: 10.1109/TVT.2018.2866414.

[10]   S. A. Busari, K. M. S. Huq, S. Mumtaz, L. Dai, and J. Rodriguez, "Millimeter-wave massive MIMO communication for future wireless systems: A survey," *IEEE Communications Surveys & Tutorials*, vol. 20, no. 2, pp. 836–869, 2018, doi: 10.1109/COMST.2017.2787460.

[11]   M. Jaber, M. A. Imran, R. Tafazolli, and A. Tukmanov, "5G backhaul challenges and emerging research directions: A survey," *IEEE Access*, vol. 4, pp. 1743–1766, 2016, doi: 10.1109/ACCESS.2016.2556011.

[12]   C.-H. Lee, S.-H. Lee, K.-C. Go, S.-M. Oh, J. S. Shin, and J.-H. Kim, "Mobile small cells for further enhanced 5G heterogeneous networks," *ETRI Journal*, vol. 37, no. 5, pp. 856–866, Oct. 2015, doi: 10.4218/etrij.15.2415.0022.

[13]   A. A. Ajani, V. K. Oduol, and Z. K. Adeyemo, "GPON and V-band mmWave in green backhaul solution for 5G ultra-dense network," *International Journal of Electrical and Computer Engineering (IJECE)*, vol. 11, no. 1, pp. 390–401, Feb. 2021, doi: 10.11591/ijece.v11i1.pp390-401.

[14]   A. Oboyerulu and O. Felix, "Comparative analysis of GPON and DSL access technologies for enhancing broadband internet penetration in Nigeria," *International Journal of Applied Information Systems*, vol. 10, no. 8, pp. 16–21, Apr. 2016, doi: 10.5120/ijais2016451466.

[15]   W. Ni, I. B. Collings, X. Wang, and R. P. Liu, "Multi-hop point-to-point FDD wireless backhaul for mobile small cells," *IEEE Wireless Communications*, vol. 21, no. 4, pp. 88–96, Aug. 2014, doi: 10.1109/MWC.2014.6882300.

[16]   X. Ge, L. Pan, S. Tu, H.-H. Chen, and C.-X. Wang, "Wireless backhaul capacity of 5G ultra-dense cellular networks," in *2016 IEEE 84th Vehicular Technology Conference (VTC-Fall)*, Sep. 2016, pp. 1–6, doi: 10.1109/VTCFall.2016.7881969.

[17]   S. Rajoria, A. Trivedi, and W. W. Godfrey, "A comprehensive survey: Small cell meets massive MIMO," *Physical Communication*, vol. 26, pp. 40–49, Feb. 2018, doi: 10.1016/j.phycom.2017.11.004.

[18]   Z. Gao, L. Dai, D. Mi, Z. Wang, M. A. Imran, and M. Z. Shakir, "MmWave massive-MIMO-based wireless backhaul for the 5G ultra-dense network," *IEEE Wireless Communications*, vol. 22, no. 5, pp. 13–21, Oct. 2015, doi: 10.1109/MWC.2015.7306533.

[19]   M. Nakamura, G. K. Tran, and K. Sakaguchi, "Interference management for millimeter-wave mesh backhaul networks," in *2019 16th IEEE Annual Consumer Communications & Networking Conference (CCNC)*, Jan. 2019, pp. 1–4, doi: 10.1109/CCNC.2019.8651725.

[20]   M. Feng and S. Mao, "Dealing with limited backhaul capacity in millimeter-wave systems: A deep reinforcement learning approach," *IEEE Communications Magazine*, vol. 57, no. 3, pp. 50–55, Mar. 2019, doi: 10.1109/MCOM.2019.1800565.

[21]   C. Saha and H. S. Dhillon, "Millimeter wave integrated access and backhaul in 5G: Performance analysis and design insights," *IEEE Journal on Selected Areas in Communications*, vol. 37, no. 12, pp. 2669–2684, Dec. 2019, doi: 10.1109/JSAC.2019.2947997.

[22]   S. G. Larew, T. A. Thomas, M. Cudak, and A. Ghosh, "Air interface design and ray tracing study for 5G millimeter wave communications," in *2013 IEEE Globecom Workshops (GC Wkshps)*, 2013, pp. 117–122, doi: 10.1109/GLOCOMW.2013.6824972.

[23]   P. Varzakas, "Optimal radio capacity for hybrid DS/SFH CDMA system in cellular radio," *Electronics Letters*, vol. 40, no. 7, 2004, doi: 10.1049/el:20040242.

[24]   W. Hao and S. Yang, "Small cell cluster-based resource allocation for wireless backhaul in two-tier heterogeneous networks with massive MIMO," *IEEE Transactions on Vehicular Technology*, vol. 67, no. 1, pp. 509–523, Jan. 2018, doi: 10.1109/TVT.2017.2739203.

[25]   3GPP TR 38.901 version 15.0.0 Release 15, "Study on channel model for frequencies from 0.5 to 100 GHz," ETSI, Techincal Report, 2018.

[26]   T. S. Rappaport *et al.*, "Millimeter wave mobile communications for 5G cellular: it will work!," *IEEE Access*, vol. 1, pp. 335–349, 2013, doi: 10.1109/ACCESS.2013.2260813.

[27]   N. Iqbal *et al.*, "Multipath Cluster Fading Statistics and Modeling in Millimeter Wave Radio Channels," no. c, pp. 1–12, 2019, doi: 10.1109/TAP.2019.2894277.

BIOGRAPHIES OF AUTHORS
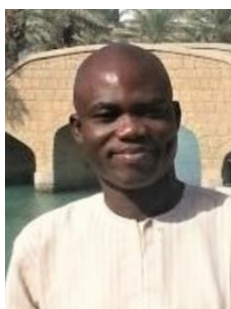
Olabode Idowu-Bismark ⓘ 🅖 sc ↻ is a Senior Lecturer at Covenant University, Ota, Nigeria. He holds a B.Eng. degree in Electrical and Electronics Engineering from the University of Benin, Nigeria and a M.Sc. in Telecommunications Engineering from Birmingham University UK. He obtained his Ph.D. in Information and Communication Engineering from Covenant University. Olabode has worked in various companies as an engineer, senior engineer, and technical manager. He is a member of the Nigerian Society of Engineers, member, MIEEE, and a COREN Registered Engineer. His research interest is in the area of mobile communication, mmWave, and MIMO communication. He has published many scientific papers in international peer-reviewed journals and conferences. He can be contacted at email: olabode.idowu-bismark@covenantuniversity.edu.ng and idowubismarkolabode@gmail.com.

Francis Idachaba ⓘ 🔗 SC ⬡ is a Professor of Communication Engineering in the Department of Electrical and Information Engineering at Covenant University Ota Ogun State. He obtained his Ph.D. in Electronics and Telecommunication Engineering from the University of Benin in Edo State Nigeria. With over 15 years in academia, he has within the last five years served as a research fellow in 2013 at the Massachusetts Institute of Technology in the US. He has over 90 publications in both journals and conferences. He is involved in the internet of things, 5G communications, and smart cities research among other interests. He is a member of the Society of Petroleum Engineers, the Nigerian Society of Engineers, and a registered Engineer in Nigeria. He can be contacted at email: francis.idachaba@covenantuniversity.edu.ng.

Aderemi Atayero ⓘ 🔗 SC ⬡ is The Covenant University Professor of Communication Engineering. He has a Bachelor of Science Degree in Radio Engineering and a Master of Science Degree in Satellite Communication Systems in 1992 and 1994 respectively. He earned his Ph.D. from the Moscow State Technical University of Civil Aviation (MSTUCA) in 2000. Atayero is a Fellow of the Science Association of Nigeria (FSAN) as well as a Senior Research Fellow of the International Association of Research Scholars and Administrators. He is a COREN Registered Engineer and member of the Institute of Electrical and Electronics Engineers (IEEE). He has published over a hundred scientific papers in both journals and conferences. His current research interests are in various aspects of Communication Engineering, including wireless sensor networks, wireless (mobile) communications, internet of things (IoT), smart cities, and cyber-physical systems. He can be contacted at email: atayero@covenantuniversity.edu.ng.